A Linear Technique to Understand Non-Normal Turbulence Applied to a Magnetized Plasma

B. Friedman* and T.A. Carter
Department of Physics and Astronomy, University of California, Los Angeles, California 90095-1547, USA

In nonlinear dynamical systems with highly nonorthogonal linear eigenvectors, linear non-modal analysis is more useful than normal mode analysis in predicting turbulent properties. However, the non-trivial time evolution of non-modal structures makes quantitative understanding and prediction difficult. We present a technique to overcome this difficulty by modelling the effect that the advective nonlinearities have on spatial turbulent structures. The nonlinearities are taken as a periodic randomizing force with time scale consistent with critical balance arguments. We apply this technique to a model of drift wave turbulence in the Large Plasma Device (LAPD) [W. Gekelman *et al.*, Rev. Sci. Inst. **62**, 2875 (1991)], where non-modal effects dominate the turbulence. We compare the resulting growth rate spectra to that obtained from a nonlinear simulation, showing good qualitative agreement.

Keywords:

Normal mode analysis – the calculation of eigenvalues and eigenvectors of a linearized dynamical system – has been used to solve many problems over the years. Despite its wide-ranging success, it has failed in important instances, particularly in predicting the onset of subcritical turbulence in hydrodynamic flows. The reason for this failure was explained in the early 1990's when Trefethen and others attributed the pitfalls of normal mode analysis to the non-normality of linear operators of dynamical systems [1, 2]. A non-normal operator has eigenvectors that are nonorthogonal to one another. One consequence of eigenvector nonorthogonality is that even when all eigenvectors decay exponentially under linear evolution, superpositions of eigenvectors can grow, albeit transiently. In other words, certain fluctuations of the laminar state can access free energy from background gradients even though normal mode fluctuations cannot. When combined with nonlinear effects, this allows for sustained subcritical turbulence. Such behavior is obscured by traditional normal mode analysis, which only effectively describes the long time asymptotic behavior of fluctuations under the action of the linear operator. Transient growth behavior, which can dominate turbulent evolution, can be discovered only through non-modal calculations.

Non-modal analysis has been embraced by the hydrodynamics community over the past two decades in the attempt to explain and predict subcritical turbulence. But the plasma community still heavily relies on normal mode analysis to inform turbulent predictions and observations, with a few notable exceptions [3–5]. Furthermore, non-modal treatments have generally been explanatory rather than predictive and have centered around the transition to turbulence in subcritical systems rather than on properties of fully-developed turbulence. This paper takes up the task of developing an approach to understand turbulent properties using only non-modal linear calculations with the goal of ultimately making quantitative predictions. Our approach is to evolve the linear solution from an ensemble of random initial conditions and calculate the average growth rate of the solutions over a specified timescale. Optimally this time scale would be the nonlinear decorrelation time of the turbulent system, but in order to enable predictive capability, we employ critical balance arguments to use a characteristic *linear* time. Since there is no obvious single linear time scale, we test several and compare the results to determine which works best. The procedure ultimately produces growth rate spectra that can be used to predict turbulent properties such as saturation levels and transport rates through mixing length arguments. While the concepts behind this technique are general enough to be applied to many nonlinear dynamical systems, the details vary for each case, so we restrict our treatment to one particular turbulence model. For this model, the technique qualitatively reproduces the turbulent growth rate spectrum of the direct nonlinear simulation fairly well, especially in comparison to the linear eigenmode spectrum.

The model we use describes pressure-gradient-driven turbulence in the uniformly magnetized, cylindrical plasma produced by the Large Plasma Device (LAPD) [6]. We use a reduced Braginskii 2-fluid model [7–11]:

$$\partial_t N = -\mathbf{v}_E \cdot \nabla N_0 - N_0 \nabla_\| v_{\|e} + S_N + \{\phi, N\}, \tag{1}$$

$$\partial_t v_{\|e} = -\frac{m_i}{m_e}\frac{T_{e0}}{N_0}\nabla_\| N - 1.71\frac{m_i}{m_e}\nabla_\| T_e + \frac{m_i}{m_e}\nabla_\|\phi - \nu_e v_{\|e} + \{\phi, v_{\|e}\}, \tag{2}$$

$$\partial_t \varpi = -N_0 \nabla_\| v_{\|e} - \nu_{in}\varpi + \{\phi, \varpi\}, \tag{3}$$

$$\partial_t T_e = -\mathbf{v}_E \cdot \nabla T_{e0} - 1.71\frac{2}{3}T_{e0}\nabla_\| v_{\|e} + \frac{2}{3N_0}\kappa_{\|e}\nabla_\|^2 T_e - \frac{2m_e}{m_i}\nu_e T_e + S_T + \{\phi, T_e\}, \tag{4}$$

where N is the density, $v_{\|e}$ the parallel electron velocity,

$\varpi \equiv \nabla_\perp \cdot (N_0 \nabla_\perp \phi)$ the potential vorticity, T_e the electron temperature, $\mathbf{v}_E$ the $\mathbf{E}\times\mathbf{B}$ velocity, and S_N and S_T density and temperature sources. All lengths are normalized to the ion sound gyroradius ρ_s, times to the ion cyclotron time ω_{ci}^{-1}, velocities to the sound speed c_s, densities to the equilibrium peak density, and electron temperatures and potentials to the equilibrium peak electron temperature. The profiles N_0 and T_{e0} and other parameters are taken from experimental measurements [10–12].

The equations are global and we retain advective nonlinearities, which are written with Poisson brackets, but we neglect other nonlinear terms. We add artificial diffusion and viscosity terms with small numerical coefficients (10^{-3}) to ensure numerical stability in nonlinear simulations, which are performed with the BOUT++ code [13]. We use periodic axial and zero value radial boundary conditions. Further details of the model, including validation studies, may be found in the references [7–11], though we mention here that the model does very well in reproducing the statistical properties of the experimentally-observed turbulence.

The nonlinear simulation reveals a fascinating property of the turbulence – it is dominated by a nonlinear instability process despite being linearly unstable to drift waves [10, 11]. The nonlinear instability, which was discovered by Drake et al. [14], works as follows: magnetic-field-aligned ($k_\parallel = 0$) convective filaments transport density across the equilibrium density gradient, setting up $k_\parallel = 0$ density filaments. These filaments are unstable to secondary drift waves, which grow on the periphery of the filaments. These drift waves, which have finite $k_\parallel$, nonlinearly couple to one another and reinforce the original convective filaments.

Although the instability is called a nonlinear instability, the first part of the mechanism – the transport of background density by the convective filaments – is a linear one. In fact, the other parts of the mechanism are driven by energetically conservative nonlinear interactions, meaning that the convective transport is the only step responsible for energy injection into the fluctuations.

Deriving an equation for the evolution of the energy from Eqs. 1-4 [10, 11], we may symbolically write

$$\frac{dE(m,n)}{dt} = \frac{dE_l(m,n)}{dt} + \frac{dE_{nl}(m,n)}{dt} \tag{5}$$

where m and n represent the azimuthal and axial Fourier mode numbers. $\frac{dE_l(m,n)}{dt}$ comes from the linear terms in Eqs. 1-4. $\frac{dE_{nl}(m,n)}{dt}$ comes from the nonlinear terms. $\frac{dE_l(m,n)}{dt}$ represents the injection (or dissipation) of energy into the fluctuations from the free energy in the equilibrium gradients. $\frac{dE_{nl}(m,n)}{dt}$ accounts for the energy exchange between fluctuations with different m, n and it is conservative: $\sum_{m,n} \frac{dE_{nl}(m,n)}{dt} = 0$. Moreover, in quasi-steady state turbulence, the rate of energy injection (or dissipation) into the fluctuations at each m, n by the linear terms must be balanced by the rate of energy removal (or deposition) from the nonlinear terms:

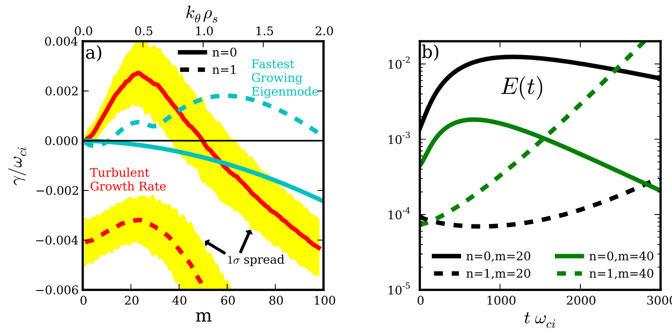

FIG. 1: a) Linear evolution of energy starting from a turbulent initial state. The $n = 0$ curves have an initial period of transient growth before exponentially decaying. b) Linear and turbulent growth rate spectra for $n = 0$ (solid lines) and $n = 1$ (dashed lines) Fourier components. The linear growth rates are those of the least stable eigenmodes, while the turbulent growth rates represent $\frac{\partial E_l}{\partial t}/2E$ from the nonlinear simulation. The shaded region marks the 1σ spread in the turbulent spectrum, obtained from the distribution of growth rates in the nonlinear simulation.

$$\gamma(m,n) \equiv \lim_{T\to\infty} \frac{1}{T}\int_0^T \frac{dE(m,n)/dt}{2E(m,n)} dt$$
$$= \lim_{T\to\infty} \frac{\mathrm{Log}\left[E(T)/E(0)\right]}{T} = 0 \quad \text{in steady state.} \tag{6}$$

From, Eqs. 5 and 6, it follows that $\gamma(m,n) = \gamma_l(m,n) + \gamma_{nl}(m,n) = 0$. The rate of energy injection $\gamma_l(m,n)$ from the equilibrium gradient into the fluctuations is a quantity of great interest [10, 15]. When positive for some wavenumber, turbulence can be sustained. Additionally, it may be used in the mixing length formula $\gamma/k_\perp^2$ to predict the turbulent saturation level, and it is proportional to the transport rate [15]. $\gamma_l(m,n)$ may be calculated from the spatial structures of the plasma state variables, so it is always well-defined, even in a turbulent plasma. We plot $\gamma_l(m,n)$ in Fig. 1 a) for both the linear and steady state turbulent stages of our nonlinear simulation. The linear stage, which occurs when fluctuations are small and exponentially growing has a time-independent $\gamma_l(m,n)$ equal to $\gamma_s(m,n)$ – the "spectral" growth rate of the fastest growing eigenmode at each m, n. During the turbulent stage, $\gamma_l(m,n)$ is time-dependent (indicated by the 1σ spread), and generally much different than $\gamma_s(m,n)$. Significantly, the turbulent γ_l is positive at $n = 0$ and low m despite the fact that all linear eigenmodes have $\gamma_s < 0$ for $n = 0$. This is a manifestation of non-normality, for in normal systems, $\gamma_l(m,n) \le \gamma_s(m,n)$. Physically, it is the manifestation of the nonlinear instability, specifically the linear part of the mechanism in which convective filaments drive density filaments from the equilibrium density gradient.

This convective transport of density filaments is akin to the paradigmatic "lift-up" mechanism in hydrodynamic shear flows whereby streamwise vortices drive streamwise streaks [1, 16]. Both are transient growth processes. We see this in our simulations by following the evolution of the energy of several m, n modes after turning off the nonlinearities in an already turbulent simulation. A few representative modes are shown in Fig. 1 b). The linear transient growth of the filamentary $n = 0$ structures is evident as their modes grow transiently before decaying exponentially at the rate of their least stable eigenmode. Such behavior is indicative of non-modal behavior. It must be since all $n = 0$ linear eigenmodes are stable. Notice also that the $n = 1, m = 20$ mode decays transiently before growing exponentially with growth rate of the most unstable eigenmode. This transient decay is also a non-modal result since $\gamma_s(n = 1, m = 20) > 0$.

Since transient growth is a purely linear phenomenon, it has been a goal of researchers to understand and predict the onset of subcritical turbulence using only linear, non-modal calculations. In our system, the turbulence is not subcritical in the traditional sense, but it has a subcritical component because $\gamma_l(m < 50, n = 0) > 0$, yet $\gamma_s(m, n = 0) < 0$. It is our goal, then, to use linear non-modal calculations to understand this behavior and to move toward predictive capability of γ_l. To accomplish this, we make the anzatz that nonlinearities randomize the turbulent spatial structure at each wavenumber on a time scale of one eddy decorrelation time, while the linearities evolve the spatial structures deterministically. From this we can calculate a non-modal $\gamma_{\mathrm{n-m}}$ spectrum, which is our prediction of the turbulent γ_l spectrum. To illustrate, we begin by taking Eqs. 1-4 and Fourier decomposing in the azimuthal and axial directions. Then, we discritize in the radial direction and approximate radial derivatives with finite differences. The resulting system of equations may be written in matrix form:

$$\mathbf{B}_{m,n}\frac{d\mathbf{v}_{m,n}(t)}{dt} = \mathbf{C}_{m,n}\mathbf{v}_{m,n}(t) - \sum_{m',n'} \mathbf{v}_{E,m-m',n-n'} \cdot \nabla_\perp \left(\mathbf{B}_{m',n'}\mathbf{v}_{m',n'}(t)\right), \tag{7}$$

where $\mathbf{v}_{m,n} = \left(N(r), v_{\|e}(r), \phi(r), T_e(r)\right)^T_{m,n}$ is the state of the system, and $\mathbf{B}_{m,n}$ and $\mathbf{C}_{m,n}$ are coefficient matrices that include the equilibrium information and finite difference coefficients. The first term on the RHS represents the linearities and the second term the nonlinearities. Note that for each m, n, there exist $4N_r$ linearly independent, but nonorthogonal eigenvectors, where N_r is the number of radial grid points. Hence forth, we drop the m, n Fourier subscripts.

In order to use non-modal analysis to calculate growth rates and other measures, one must choose a norm and inner product with which to work. While any choice of inner product is possible, a physically relevant one such as an energy inner product is generally preferred [2–4]. Recall that the inner product of two vectors may be written $\langle \mathbf{x}, \mathbf{y}\rangle = \mathbf{y}^\dagger \mathbf{M}\mathbf{x}$. We choose $\mathbf{M}$ so that $||\mathbf{v}||^2 = \langle \mathbf{v}, \mathbf{v}\rangle = E$. Furthermore, it is convenient in computations to use the L_2-norm, $||\mathbf{u}||_2^2 = \sum_i |u_i|^2$. This can be accomplished through the change of variables $\mathbf{u} = \mathbf{M}^{\frac{1}{2}}\mathbf{v}$. Then the linear portion of Eq. 7 becomes

$$\frac{d\mathbf{u}}{dt} = \mathbf{A}\mathbf{u}, \quad \text{where } \mathbf{A} = \mathbf{M}^{\frac{1}{2}}\mathbf{B}^{-1}\mathbf{C}\mathbf{M}^{-\frac{1}{2}}. \tag{8}$$

The solution of Eq. 8 is $\mathbf{u}(t) = e^{\mathbf{A}t}\mathbf{u}(0)$, which depends on the initial condition $\mathbf{u}(0)$. For purposes of turbulent growth rate prediction, we are interested in the behavior of $G(t) = E(t)/E(0) = ||\mathbf{u}(t)||^2/||\mathbf{u}(0)||^2$ and its rate of growth.

It is common practice in normal mode analysis to look for the least stable eigenmode. For the non-modal case, it is common to study the properties of $G_{\max}(t) = ||e^{\mathbf{A}t}||$ because if this is greater than unity at any time, fluctuations may be amplified, leading to subcritical turbulence [2, 17]. However, it can be misleading to study only $G_{\max}(t)$ when predicting specific properties of turbulence because $G_{\max}(t)$ is only the upper envelope of all possible $G(t)$ curves. No one particular initial condition $\mathbf{u}(0)$ evolves along $G_{\max}(t)$. Furthermore, it isn't obvious what kind of spatial structure or structures will come to dominate a turbulent system. In non-normal systems, unlike in normal systems, optimal structures don't amplify themselves, rather, they evolve while increasing the total fluctuating energy.

We contend that the key to understanding and predicting turbulent properties through non-modal analysis is to successfully model the effect that the nonlinearities have on the transient linear processes. To this effect, we note that the advective nonlinearity in Eq. 7 has the form of the state vector divided by a time $\tau_{nl} \sim (v_E k_\perp)^{-1}$. This nonlinear time scale is generally associated with the eddy turnover or decorrelation time. We therefore present a heuristic model of the nonlinearities as a randomizing force that acts on this characteristic nonlinear time scale. Specifically, we start with an ensemble of random initial conditions, evolve them linearly for a time τ_{nl}, then take the time and ensemble averaged growth rate of these curves. This procedure calculates the average growth rate of the turbulence as if the turbulence evolved linearly for a time τ_{nl}, randomized, and then repeated. Now, this procedure does not require actual linear simulations from an ensemble of random initial conditions. To see this, recall that the time evolution of the energy from an initial condition is

$$E(t) = ||e^{\mathbf{A}t}\mathbf{u}(0)||^2 = e^{\mathbf{A}t}\mathbf{u}(0)\mathbf{u}^\dagger(0)e^{\mathbf{A}^\dagger t}. \tag{9}$$

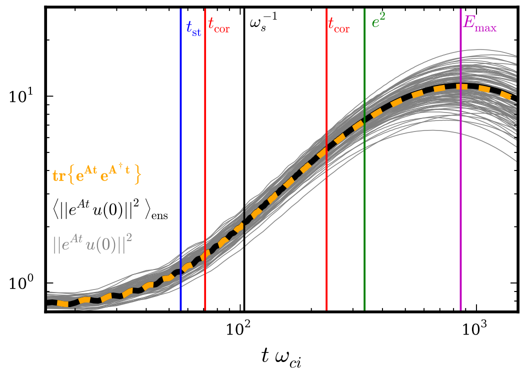

FIG. 2: An ensemble of initially randomized growth ratio curves (solid gray lines, with the solid black line their average, and the dashed orange line the average as calculated from Eq. 10). The vertical lines indicate various linear time scales.

If the $\mathbf{u}(0)$ in the ensemble are random with uncorrelated components and normalized to unity, it follows that [3]

$$\langle E(t)/E(0)\rangle_{\rm ens} = \frac{1}{4N_r}\mathrm{tr}\{e^{\mathbf{A}t}e^{\mathbf{A}^\dagger t}\}. \tag{10}$$

We show the validity of this statistical averaging by plotting 1000 ensemble curves in Fig. 2 along with their expected average from Eq. 10 and their actual average, which line up perfectly. One point to note is that in global equation sets like ours, where we discritize and use finite differences in the radial direction rather than a Fourier decomposition, randomizing $\mathbf{u}(0)$ amounts to setting the initial k_r spectrum to a step function that goes to zero at the Nyquist wavenumber. This means that $\langle E(t)/E(0)\rangle_{\rm ens}$ may depend on N_r, so we must be careful in choosing N_r for this analysis. We choose N_r such that the grid spacing equals ρ_s, the general Nyquist wavenumber of drift wave simulations [18].

Mathematically, our procedure is to calculate $\gamma_{\rm n-m}$ by the following formula:

$$\gamma_{\rm n-m} = \frac{1}{\tau_{nl}}\int_0^{\tau_{nl}} \frac{\frac{\partial E(t)}{\partial t}}{2E(t)}dt = \frac{1}{2\tau_{nl}}\mathrm{Log}\left[\frac{E(\tau_{nl})}{E(0)}\right] \tag{11}$$

where $E(t)$ is the ensemble averaged energy calculated from Eq. 10, and $E(0) = 1$ by our normalization. In order to move toward predictive capability, we must estimate τ_{nl} with only knowledge of linear (modal or non-modal) information. We thus invoke the conjecture of *critical balance*, which posits that the nonlinear time scale equals the linear time scale at all spatial scales [5]. This follows from the previously derived steady-state result: $\gamma_l = -\gamma_{nl}$.

Now there are several linear time scales that we may choose to test. We label these times in Fig. 2 for the case of $n = 0, m = 20$. The first linear time is the linear eigenmode frequency, labeled ω_s^{-1}. However, $\omega_s = 0$ for $n = 0$ linear eigenmodes, so we are forced to use ω_s for the fastest growing $n = 1$ eigenmode at each m to get a meaningful time scale. Second is the parallel free-streaming time of the electrons $t_{\rm st} = L_\parallel/v_{te}$ often cited in critical balance arguments [19]. Third is the time before modal effects take over, which can be approximated as the time when $E(t)$ turns over. As seen in Fig. 1, $E(t)$ can be either a maximum or minimum before turning over. We label this time $E_{\rm max}$. Fourth, we use the steady-state condition $\gamma_l = -\gamma_{nl}$ and the approximation $\tau_{nl} \sim 1/|\gamma_{nl}|$ to get $\tau_{nl} = 1/|\gamma_{\rm n-m}|$. Inserting this into Eq. 11 gives

$$\mathrm{Log}\left[E(1/\gamma_{\rm n-m})\right] = \pm 2 \;\rightarrow E(1/\gamma_{\rm n-m}) = e^{\pm 2}. \tag{12}$$

In other words, we find the time at which $E(t)$ grows to the value of e^2 or decays to the value of e^{-2}, and then use this time to get $\gamma_{\rm n-m}$. We label this time e^2. In Fig. 2, we also indicate two times labeled $t_{\rm cor}$, which when inserted into Eq. 11 give the "correct" $\gamma_l(m = 20, n = 0)$ calculated directly from the nonlinear simulation.

In Fig. 3, we compare the γ_l spectrum from the nonlinear simulation to γ_{n-m} from the non-modal procedure using the four different linear time scales. We also show γ_s for reference. All of the non-modal growth rates are positive at $n = 0$ for low m, like γ_l from the simulation and unlike γ_s, indicating that the non-modal analysis can reveal what normal mode analysis cannot in this turbulent system. Furthermore, the choice of linear time scale does not significantly affect the qualitative picture.

On the other hand, the non-modal analysis does not always predict complete stability at $n = 1$ for all choices of linear time scale, but it does indicate that $n = 1$ modes can dissipate rather than inject fluctuation energy despite the presence of unstable linear eigenmodes. Interestingly, the linear eigenmode time scale ω_s^{-1} gives the best match to γ_l, however, this may not be a general result.

In summary, we present a procedure for calculating the turbulent growth rate spectrum using non-modal linear calculations. In the case of an LAPD experiment, this procedure captures the behavior of a nonlinear instability that dominates the dynamics of the turbulence. In general, non-modal analysis is difficult to quantify and make predictive, but using some simple nonlinear modelling, we have shown that it may be possible. Future studies will attempt to test this procedure on other non-normal turbulence models and to see if it can predict critical parameters for subcritical turbulent onset.

This work was supported by the National Science Foundation (Grant PHY-1202007)

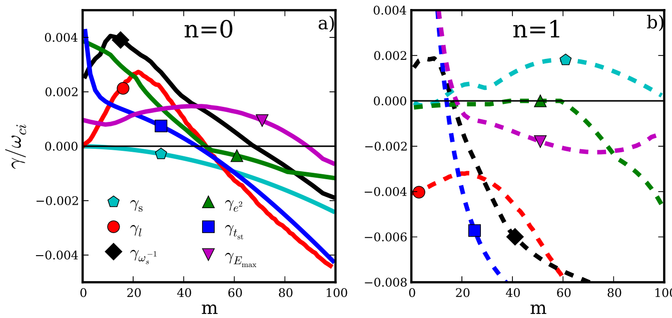

FIG. 3: The growth rate spectra of the spectral growth rate γ_s, turbulent simulation growth rate γ_l, and growth rates calculated from the non-modal procedure in Eq. 11. The growth rates as a function of m for a) $n = 0$ and b) $n = 1$.

* Electronic address: `friedman@physics.ucla.edu`

[1] L. N. Trefethen, A. E. Trefethen, S. C. Reddy, and T. A. Driscoll, Science **261**, 578 (1993).
[2] P. J. Schmid, Annu. Rev. Fluid Mech. **39**, 129 (2007).
[3] S. J. Camargo, M. K. Tippett, and I. L. Caldas, Phys. Rev. E **58**, 3693 (1998).
[4] E. Camporeale, D. Burgess, and T. Passot, The Astrophysical Journal **715**, 260 (2010).
[5] A. A. Schekochihin, E. G. Highcock, and S. C. Cowley, Plasma Phys. Control. Fusion **54**, 055011 (2012).
[6] W. Gekelman et al., Rev. Sci. Inst. **62**, 2875 (1991).
[7] P. Popovich, M. V. Umansky, T. A. Carter, and B. Friedman, Phys. Plasmas **17**, 102107 (2010).
[8] P. Popovich, M. V. Umansky, T. A. Carter, and B. Friedman, Phys. Plasmas **17**, 122312 (2010).
[9] M. V. Umansky, P. Popovich, T. A. Carter, B. Friedman, and W. M. Nevins, Phys. Plasmas **18**, 055709 (2011).
[10] B. Friedman, T. A. Carter, M. V. Umansky, D. Schaffner, and B. Dudson, Phys. Plasmas **19**, 102307 (2012).
[11] B. Friedman, T. A. Carter, M. V. Umansky, D. Schaffner, and I. Joseph, Phys. Plasmas **20**, 055704 (2013).
[12] D. A. Schaffner et al., Phys. Rev. Lett. **109**, 135002 (2012).
[13] B. D. Dudson, M. V. Umansky, X. Q. Xu, P. B. Snyder, and H. R. Wilson, Computer Physics Communications , 1467 (2009).
[14] J. F. Drake, A. Zeiler, and D. Biskamp, Phys. Rev. Lett. **75**, 4222 (1995).
[15] P. W. Terry, D. A. Baver, and S. Gupta, Phys. Plasmas **13**, 022307 (2006).
[16] J. A. Krommes, Plasma Phys. Control. Fusion **41**, A641 (1999).
[17] L. N. Trefethen and M. Embree, *Spectra and Pseudospectra: The Behavior of Nonnormal Matrices and Operators*, Princeton Univ. Press, 2005.
[18] B. D. Scott, Phys. Fluids B **4**, 2468 (1992).
[19] M. Barnes, F. I. Parra, and A. A. Schekochihin, Phys. Rev. Lett. **107**, 115003 (2011).